CORA Cork Open Research Archive
Cartlann Taighde Oscailte Chorcaí

Title	Characterization of primary organic aerosol from domestic wood, peat, and coal burning in Ireland
Authors	Lin, Chunshui;Ceburnis, D.;Hellebust, Stig;Buckley, Paul;Wenger, John C.;Canonaco, Francesco;Prévôt, André Stephan Henry;Huang, Ru-Jin;O'Dowd, Colin D.;Ovadnevaite, Jurgita
Publication date	2017-08-17
Original Citation	Lin, C., Ceburnis, D., Hellebust, S., Buckley, P., Wenger, J., Canonaco, F., Prévôt, A. S. H., Huang, R.-J., O'Dowd, C., Ovadnevaite, J. (2017) 'Characterization of primary organic aerosol from domestic wood, peat, and coal burning in Ireland', Environmental Science and Technology, 51(18), pp.10624-10632. doi:10.1021/acs.est.7b01926
Type of publication	Article (peer-reviewed)
Link to publisher's version	10.1021/acs.est.7b01926
Rights	© 2017, American Chemical Society. All rights reserved. This document is the Accepted Manuscript version of a Published Work that appeared in final form in Environmental Science and Technology, after peer review and technical editing by the publisher. To access the final edited and published work see http://pubs.acs.org/doi/abs/10.1021/acs.est.7b01926
Download date	2026-11-14 14:56:32
Item downloaded from	https://hdl.handle.net/10468/4921

UCC
University College Cork, Ireland
Coláiste na hOllscoile Corcaigh

Environmental Science & Technology

Subscriber access provided by UNIV COLL CORK

Article

Characterization of primary organic aerosol from domestic wood, peat, and coal burning in Ireland

Chunshui Lin, Darius Ceburnis, Stig Michael Hellebust, Paul Buckley, John Charles Wenger, Francesco Canonaco, Andre S.H. Prevot, Ru-Jin Huang, Colin O'Dowd, and Jurgita Ovadnevaite

Environ. Sci. Technol., **Just Accepted Manuscript** • DOI: 10.1021/acs.est.7b01926 • Publication Date (Web): 17 Aug 2017

Downloaded from http://pubs.acs.org on August 23, 2017

Just Accepted

"Just Accepted" manuscripts have been peer-reviewed and accepted for publication. They are posted online prior to technical editing, formatting for publication and author proofing. The American Chemical Society provides "Just Accepted" as a free service to the research community to expedite the dissemination of scientific material as soon as possible after acceptance. "Just Accepted" manuscripts appear in full in PDF format accompanied by an HTML abstract. "Just Accepted" manuscripts have been fully peer reviewed, but should not be considered the official version of record. They are accessible to all readers and citable by the Digital Object Identifier (DOI®). "Just Accepted" is an optional service offered to authors. Therefore, the "Just Accepted" Web site may not include all articles that will be published in the journal. After a manuscript is technically edited and formatted, it will be removed from the "Just Accepted" Web site and published as an ASAP article. Note that technical editing may introduce minor changes to the manuscript text and/or graphics which could affect content, and all legal disclaimers and ethical guidelines that apply to the journal pertain. ACS cannot be held responsible for errors or consequences arising from the use of information contained in these "Just Accepted" manuscripts.

ACS Publications

Environmental Science & Technology is published by the American Chemical Society. 1155 Sixteenth Street N.W., Washington, DC 20036

Published by American Chemical Society. Copyright © American Chemical Society. However, no copyright claim is made to original U.S. Government works, or works produced by employees of any Commonwealth realm Crown government in the course of their duties.

Characterization of primary organic aerosol from domestic wood, peat, and coal burning in Ireland

Chunshui Lin[a,b], Darius Ceburnis[a], Stig Hellebust[c], Paul Buckley[c], John Wenger[c], Francesco Canonaco[d], André Stephan Henry Prévôt[d], Ru-Jin Huang[a,b,d,], Colin O'Dowd[a,*], and Jurgita Ovadnevaite[a]*

[a]School of Physics and Centre for Climate and Air Pollution Studies, Ryan Institute, National University of Ireland Galway, University Road, H91CF50, Galway, Ireland

[b] State Key Laboratory of Loess and Quaternary Geology and Key Laboratory of Aerosol Chemistry and Physics, Institute of Earth Environment, Chinese Academy of Sciences, 710061, Xi'an, China

[c]Department of Chemistry and Environmental Research Institute, University College Cork, T23XE10, Cork, Ireland

[d]Laboratory of Atmospheric Chemistry, Paul Scherrer Institute (PSI), 5232 Villigen, Switzerland

ABSTRACT: An Aerosol Chemical Speciation Monitor (ACSM) was deployed to study the primary non-refractory submicron particulate matter emissions from burning of commercially available solid fuels (peat, coal, and wood) typically used in European domestic fuel stoves. Organic mass spectra (MS) from burning wood, peat, and coal were characterized and inter-compared for factor analysis against ambient data. The reference profiles characterized in this study were used to estimate the contribution of solid fuel sources, along with oil combustion, to ambient pollution in Galway, Ireland using the multilinear engine (ME-2). During periods influenced by marine air masses, local source contribution had dominant impact and non-sea spray primary organic emissions comprised 88% of total organic aerosol mass, with peat burning found to be the greatest contributor (39%), followed by oil (21%), coal (17%), and wood (11%). In contrast, the resolved oxygenated organic aerosol (OOA) dominated the aerosol composition in continental air masses, with contributions of 50%, compared to 12% in marine air masses. The source apportionment results suggest that the use of domestic solid fuels (peat, wood, and coal) for home heating is the major source of evening/night-time particulate pollution events despite their small use.

1. INTRODUCTION

Ambient particulate matter (PM) adversely affects human health[1, 2] and has been credited with a more positive effect on climate through directly scattering or absorbing solar radiation and indirectly acting as cloud condensation nuclei[3], both leading to a partial negation of global warming induced by greenhouse gas emissions. In Ireland, domestic coal burning was the cause of numerous air pollution events in the 1980s which led to increased mortality rates[4]. The introduction of the ban on marketing, sale, and distribution of bituminous (smoky) coal in Dublin in 1990, which was subsequently extended to urban areas with a population over 15,000, resulted

in significant reductions in black smoke concentration and noticeable improvements in air quality[5, 6]. However, a recent study in the city of Cork, Ireland[7], using polar organic compounds to estimate the contribution of domestic solid fuel (DSF) combustion, indicates that despite the ban on bituminous coal, DSF is still the major source of $PM_{2.5}$ organic carbon (0.6-23.7 $\mu g/m^3$) during winter (contributing around 75% to total $PM_{2.5}$). Thus, the ban on bituminous coal alone may not be enough since peat and wood emit similar or higher amounts of PM when burned. In fact, according to the report from International Energy Agency (2013)[8], the annual consumption of bituminous coal in Ireland was 404 kt in 2013, while annual peat consumption was 611 kt, which makes peat one of the most commonly used solid fuels. In contrast, the annual consumption of wood for domestic heating was only 34 kt in 2015. Different types of DSF have different emissions factors that are dependent on the type of fuel and burning conditions[9-11]. However, developing a way to identify and evaluate the contribution of DSF burning to particulate matter with high time resolution is limited.

The identification of specific marker compounds in aerosol particles produced from different solid fuels and the use of markers for subsequent evaluation of the DSF contribution to airborne pollution has been reported by Kourtchev et al.[7] Polar organic maker compounds (i.e. levoglucosan, galactosan, and mannosan) determined by GC/MS and levoglucosan/OC ratio derived from combustion experiments of coal, peat, and wood were used to identify and evaluate their contributions to ambient PM[7]. However, GC/MS suffers from low time resolution (6 h) and levoglucosan/OC ratio might differ greatly under different burning conditions which limit this tracer approach. Recently, the Aerosol Mass Spectrometer (AMS), which determines the chemical composition and concentration of submicron aerosols on-line and at high time resolution has proved to be a robust tool for evaluating the contribution of various sources[12-17].

Based on thermal vaporization and electron impact, AMS classifies OA by mass spectrometric fingerprint rather than individual specific marker compounds[18]. Several major components of OA have been identified through positive matrix factorization (PMF) analysis of AMS mass spectra such as hydrocarbon-like (HOA), biomass burning (BBOA), oxygenated (OOA) and several other primary OA[19-21]. Direct AMS measurement of OA from various primary emissions can help understand the MS signatures of different primary OA sources and thus help the interpretation of AMS data. Emissions from motor vehicles[22, 23], meat cooking[24], and solid fuels[10, 25, 26] have been intensively studied and compared in terms of their AMS mass spectral signatures. However, the source profiles may differ with fuel types and combustion conditions, and relevant studies are very scarce, hindering the efforts for a better apportionment of sources with PMF-AMS. Healy et al.[25] and Dall'Osto et al.[26] carried out a series of experiments on wood, smokeless coal and peat burning in an open-door grate using ATOFMS (aerosol time-of-flight mass spectrometer) and HR-ToF-AMS (high -resolution time-of-flight aerosol mass spectrometer), respectively, which provides high mass resolution characterization of emitted PM. Wang et al.[9] characterized OA formation during pulverized coal combustion in a drop-tube furnace. Zhou et al.[11] studied the evolution of OA from burning different types of coal in a typical Chinese stove using an Aerosol Chemical Speciation Monitor (ACSM, a compact version of AMS)[27]. However, to the best of our knowledge, direct Q-ACSM measurements and comparison of domestic wood, peat, and coal burning have not been reported which should get more attention for their significant impacts on air quality in Ireland and other places (e.g. the UK and Finland) where these fuels are popular for domestic heating[6, 7, 25, 26].

In this study, seven solid fuel samples including dry wood (15%-20% moisture, DW), wet wood (>20% moisture, WW), dry raw peat (DP), wet raw peat (WP), peat briquettes (PB),

bituminous (smoky) coal (SC) and ovoids (smokeless, based on anthracite) coal (SLC) were burned in a typical residential stove in Ireland. Characterization of PM emitted from burning these samples was conducted using an ACSM. OA was found to be the major contributor to the total sub-micron non-refractory ($NR\text{-}PM_1$) aerosol particles. Mass spectral signatures of OA from each fuel type were obtained at unit mass resolution and compared. These signatures were used to apportion ambient OA measured by ACSM in Galway, Ireland to estimate the relative contribution of each type of fuel to air pollution and characterize their emission and formation process by comparing the influence of continental and marine air masses.

2. EXPERIMENTAL SECTION

Solid-fuel types. Wood (oak), raw peat, peat briquettes, bituminous (smoky) coal and smokeless coal ovoids were purchased locally in County (Co.) Tipperary, where the burning experiments were performed. Peat products are locally produced while smoky coal is imported from Colombia (78% of the coal in Ireland is imported from Colombia in 2014; SEAI 2016). Smokeless coal (ovoids) is purchased from ArignaBiofuels (based in Ireland) where coal is roasted, blended with other biomass products and briquetted as ovoids. Stored, dried wood had a moisture content less than 20%. Wet wood had a moisture content from 20% up to 40%. Peat is an accumulation of partially decayed vegetation and is the first step for the formation of coal. Raw peat is cut from peatlands while peat briquettes are compressed peat[28]. Raw peat was dry when purchased and was exposed to the outdoor atmosphere to achieve wet raw peat. Smoky coal and smokeless coal were directly burned as they are more water resistant.

Fingerprinting experiment set-up. The solid fuel burning experiments were performed using a solid fuel stove located in a cottage in Co. Tipperary from January 16 to 21 2016 with an

92 average ambient temperature of 6 ±3 °C and RH of 92±5%. A schematic of the stove and
93 sampling system is provided in Scheme S1. Each type of sampling fuel was continuously burned
94 for at least 1 hours with a total use of each type of fuel >5kg. The stove was cleared of residue
95 following combustion of each fuel sample. An ACSM (Aerodyne Research Inc.) was used to
96 characterize the chemical composition of the NR-PM_1 and obtain unique mass spectral signatures
97 of aerosols produced from burning each of the solid fuels. In the ACSM[27], nafion dried
98 submicron particles sampled through the inlet are deposited on the heated surface (600 °C), and
99 only the NR-PM_1 are vaporized and ionized by the ion source. The resulting ions are analyzed by
100 quadrupole mass spectrometer. Black carbon and other refractory components are not analyzed
101 by ACSM. The time resolution of ACSM for ambient measurement is usually set at ~15-30
102 minutes due to the low concentration, while in this direct fuel combustion measurement, it was
103 set at ~1 minute (1 set of sample and filter cycle) for the high aerosol emission (10-500 μg/m^3)
104 during the sampling period. The emissions from the 1 h burning were averaged to get the relative
105 mass contribution and mass spectral signatures of organic aerosol for each type of fuel.

106 **Ambient aerosol measurements in Galway.** The ambient aerosol measurements were
107 conducted in the National University of Ireland Galway's Center of Climate and Air Pollution
108 Studies (53.28°N and 9.06°W) from 17th October 2015 to 23rd November 2015. This site is
109 located adjacent to and east off the main urban residential area and at least 200 meters away from
110 the main road to avoid the direct influence from traffic. Ambient air was drawn from a height of
111 around 6 m above the ground through a tube at a flow rate at 3 LPM. A sub-stream of ~85
112 ml/min was analyzed by ACSM at a time resolution of 30 minutes. Meteorological data recorded
113 at the engineering building (1 km from the monitoring site) was used to compare and analyze the
114 origin and transport of aerosol in this study.

115

116 **Data analysis.** In this study, we employ ME-2[29, 30, 31] within the SoFi software package (version
117 6.1), an Igor-based software, for source apportionment. A detailed description of ME-2 and the
118 software package can be found in Canonaco et al.[29]. Briefly, in a typical PMF algorithm where a
119 measured matrix X can be deconvolved into two matrices (G and F) and the remaining residue
120 matrix (E), multiple combinations of G and F due to rotational ambiguity can lead to
121 mathematically meaningful but not interpretable PMF solutions especially when factors show
122 temporal covariations. An *a-value* approach within ME-2 has been successfully used to explore
123 the rotational ambiguity for online and offline data set where users can direct the algorithm
124 towards environmentally reasonable rotations by constraining reference factor profiles (currently
125 the case) or time series based on priori information.[17, 32, 33] The *a-value* determines the extent to
126 which a reference profile is allowed to vary (e.g. an *a-value* of 0.1 allows a variability of 10%).
127 In this study, the pollution events mostly happened during eveing/nighttime, indicating their
128 emission sources from domestic heating. Thus, we conducted the source apportionment by
129 constraining the primary components, i.e., oil (HOA), peat, coal, and wood using the *a-value*
130 approach and allowed for one additional free factor representing OOA. HOA reference profile,
131 taken from Crippa et al.[21], usually represents emission profile from traffic.[34, 35] However, oil
132 burning has similar particulate emissions to that of traffic emission in terms of mass spectra as
133 indicated in the diesel burning work by Schneider et al.[23] and the vehicles chase study by
134 Canagaratna et al.[22] Actually, oil burning for domestic heating is quite popular in Galway,
135 Ireland (around 85% of the non-natural gas and non-electricity households) based on the census
136 data from Central Statistics Office on the households by the type of central heating (CSO)[36]
137 (Figure S1). The night time peaks of HOA (Figure 4a and 4b) indicates its source from domestic

heating, HOA is, therefore, denoted as oil burning thereafter. The *a value* of 0.1 (*a value* of 0-0.2 was explored, more information is provided in Section **OA source apportionment**) was used for all primary factors (oil, peat, coal, and wood).

3. RESULTS AND DISCUSSION

Relative fraction of solid fuels burning NR-PM_1 emissions. Organics constitute the largest fraction of total NR-PM_1 emissions from burning fuels (e.g. ~98% for dry wood, ~91% for peat briquettes, and ~94% smoky coal) except for the smokeless coal (~26%) (Figure S2). For the latter, chloride is the major component of the aerosol particles, with a value of about 53%, followed by organics (26%), sulfate (11%), and ammonium (8%). Burning conditions have minor effects on the relative contribution of ACSM species by comparing dry and wet wood, dry and wet raw peat. In contrast, the compositions of fuel type result in differences in contributions to NR-PM_1 mass between different types of fuels. For example, wood burning emissions contain little sulfate and little ammonium (~0.3%) while all types of peat burning emissions have higher levels of sulfate, with around 5% of the total NR-PM_1 mass being sulfate for peat briquettes.

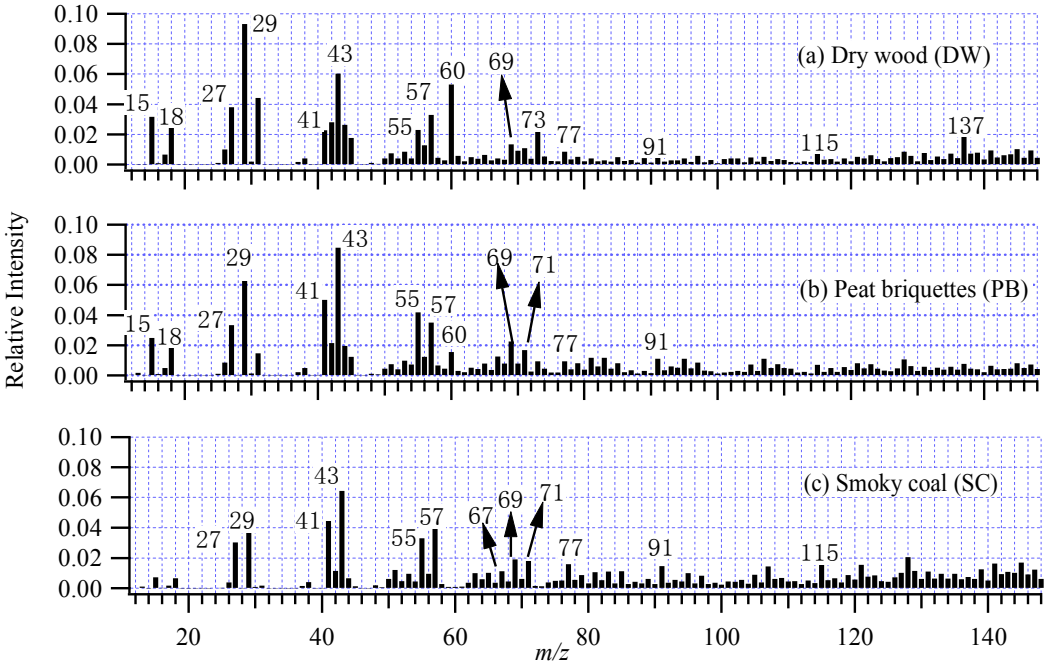


Figure 1. Normalized mass spectra of organics from the combustion of (a) dry wood; (b) peat briquettes; (c) smoky coal.

ACSM mass spectra profiles of different fuels. Averaged normalized ACSM unit mass resolution (UMR) mass spectra (MS) of OA particles obtained for dry wood, peat, and coal are shown in Figure 1. All three MS are dominated by C_nH_{2n+1} (29, 43, 57, 71…) and C_nH_{2n-1} (27, 41, 55, 69…), indicating the large contribution from saturated alkanes, alkenes, and also possible cycloalkanes in the primary OA emissions from wood, peat, and coal. However, the MS profile patterns and signals at specific m/z (e.g. m/z 60) of different fuels vary significantly corresponding to the composition of the fuels. For example, the most prominent ion in wood burning aerosol MS profile is the signal at *m/z* (mass to charge ratio) 29, followed by *m/z* 43 while *m/z* 43 is the most abundant ion in peat emissions, followed by *m/z* 29. In contrast, *m/z* 43 and *m/z* 41 are the most abundant ions in coal emissions MS. In addition, there was a relatively

higher contribution from heavier ions (>100) in the coal emission spectra most likely from PAH emissions if compared to the peat and wood spectra.

Wood. The prominent signals at *m/z* 29 and 43 in wood emissions (Figure 1a) are consistent with the previous reports using HR-ToF-AMS.[24] The large presence of CHO^+ and $C_2H_3O^+$ in HR-ToF-AMS are found to be responsible for the high signal at *m/z* 29 and *m/z* 43, respectively[24]. Mass fragments at *m/z* 60 are often regarded as marker fragments for wood burning aerosols[37] which mainly arise from the thermal decomposition of cellulose, the pyrolysis of which produces levoglucosan. The electron impact ionization of levoglucosan shows intense signals at *m/z* 60.[26] Fragment *m/z* 44 (CO_2^+, strongly influenced by di or polycarboxylic acids), a marker for OOA,[38] which arises together with *m/z* 18 (which is set to equal to *m/z* 44 in the fragmentation table as in the Q-AMS) contributes to around 2% of total BBOA signal[39, 40]. Fragment *m/z* 29 has the highest fraction of the signal in the dry wood profile. However, it is not a unique marker for wood burning due to its presence in all other fuel profiles. These characteristics are consistent with other UMR MS of OA from pine burning and PMF results of ambient OA data.[10, 37] Wet wood profile shows a higher contribution from larger *m/z* fragments especially at *m/z* 137 (Figure S3) which may be due to the fact that wet wood has a lower burning temperature which leads to incomplete combustion. Despite the differences between dry wood and wet wood profile, wood marker fragments *m/z* 60, 73 and 137 are still prominent. The MS signal fractions of *m/z* >80 for dry wood are 31% which implies that primary OA from wood burning contains high molecular weight organic compounds. This high fraction is consistent with the previous fingerprinting experiment reported by He et al.[24] in which high signal fractions of *m/z* >100 could reach 13%. However, the absolute amount is strongly influenced by the

transmission function applied in the ACSM in which small errors in the higher m/z range can cause the behavior of slowly increasing calculated signal at m/z above 100.

Peat. MS of primary OA from peat shows the highest signal fraction at *m/z* 43 (Figure 1b), which is consistent with the HR-ToF-AMS measurement of open grate peat burning[26] and ToF-ACSM measurement of peat burning in closed chamber[41]. Ions at *m/z* 43 are dominated by $C_3H_7^+$ in peat emissions while $C_2H_3O^+$ dominate the same nominal ions in wood emissions in HR-ToF-AMS[26]. $C_xH_y^+$ type ions make up 71 % of peat MS, which implies high fraction of hydrocarbon in peat emissions[26]. In addition, typical aromatic ion series at *m/z* 77 and 91 are present in the peat MS and are more prominent than that in wood MS. The presence of *m/z* 60 in peat MS profiles is due to the incomplete decay of vegetation which contains cellulose.[42] Cellulose is one of the most common chemical substances that exist in peat.[42] Although these ion series in peat profile are not as prominent as in the wood profile, ions at *m/z* 60 are enough to distinguish the peat MS profile from coal and oil whose formation involves a complete decay of vegetation. For example, HOA from traffic typically has the most prominent peak at *m/z* 57, characteristic of saturated hydrocarbons, but no signal at *m/z* 60.[20, 43] High similarity in MS profiles for dry, wet raw peat and peat briquettes (R^2>0.95) can be observed which suggests that the state of the peat (raw, wet, shredded and compressed into briquettes) does not make a difference to the OA mass spectra (Figure S4). The MS signal fractions of *m/z* > 80 for peat are 34% which is slightly higher than wood, indicating high molecular weight compounds are forming in peat.

Coal. The burning of smoky coal visibly produces a larger amount of black carbon than smokeless coal. However, the mass spectral signatures of smoky and smokeless coal appear very similar (Figure S5), both with large contribution from heavier ions. The similarity in MS patterns between smoky and smokeless coal indicates that the compositions in ovoids responsible for the

emission of primary OA are similar to that of smoky coal. The strongest peak in coal MS is the signal at *m/z* 43, followed by *m/z* 41 (Figure 1c). This is similar to peat and consistent with a previous HR-ToF-AMS measurement of emissions from open grate coal burning.[26] $C_xH_y^+$ type ions dominate the MS of coal with a fraction of 71% which is the same as peat MS profile.[26] Coal is formed through a process called "coalification"[44] when peat is physically and chemically altered as a result of bacterial decay, compaction, heat and time. No signal at *m/z* 60 was observed for smoky coal MS (Figure 1c) which might be due to the complete decomposition of cellulose in the formation of coal. In contrast, *m/z* 60 is slightly elevated in ovoids MS which might be due to its complex composition that contains biomass. The absence of *m/z* 60 distinguishes smoky coal MS from contemporary biomass burning. In addition, the signal at *m/z* 57 is slightly higher than *m/z* 55 in coal profile while the opposite is the case for peat, indicating that coal has more saturated hydrocarbon than peat. Further, fragments at *m/z* 77, 91 and 115 are stronger in coal MS than in peat MS likely due to the high fraction of aromatic compounds in coal. The signal fractions of *m/z* > 80 are 51% which is significantly higher than wood and peat.

Differences between ACSM profiles and implications for PMF analysis. The differences between the MS shown in Figure 1 are compared by plotting the relative differences of individual m/z values compared to peat (i.e. (f(m/z, wood/coal) - f(m/z, peat))/f(m/z, peat), Figure S6). The peat MS was chosen as the reference MS due to the fact peat is the middle evolution state between wood and coal. Wood and peat MS show moderate similarity with the correlation value R^2 of 0.69 (Table S2). Differences at values of m/z 29, 31, 41, 60, 73, 83, 96, and 137 are mainly responsible for the discrepancy. Higher values of m/z 29, 31, 60, 73, 137 (positive relative difference for wood) are observed for wood while higher values of m/z 41, 83, 96 (negative relative difference) are observed for peat. Coal and peat MS also show moderate

similarity with R^2 being 0.77. Higher values at m/z 29, 31, 45, 60, 73 for peat and higher values at m/z > 115 for coal contribute mainly to the discrepancy. The differences in intensities at the m/z values mentioned above are expected to play an important role in PMF to separate OA emissions from wood, peat, and coal.

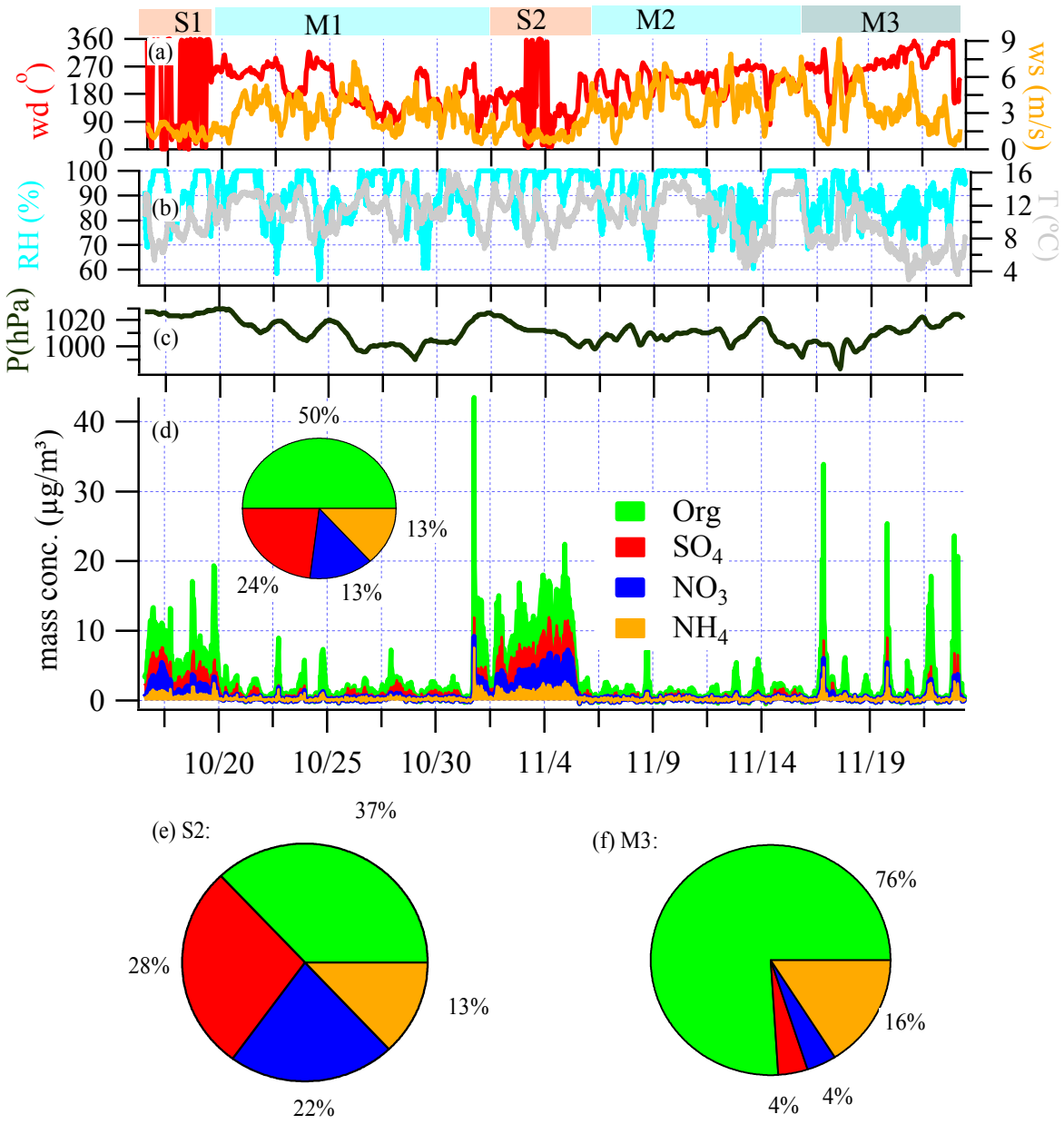
For the comparison between MS profiles of all the burning sources in this study and PMF factors of ambient measurement from literature, R^2 were calculated and summarized in Table S2. The dry and wet raw peat MS shows a good inter-correlation with R^2 being 0.98 which was higher than that between dry wood and wet wood (R^2=0.91), indicating wood burning emissions are more influenced by moisture. Smoky coal and smokeless coal show the poorest inter-correlation (R^2=0.78) which is in part due to the production process of smokeless coal from smoky coal that leaves out most of the volatile content in smoky coal responsible for the high smoke output. In fact, the signal fractions in the range *m/z* > 80 for smokeless coal MS are 40.9% which is less than that of smoky coal (51.3%). The discrepancy in the MS between smoky coal and smokeless coal can also be explained by complicated compositions of ovoids which is blended with biomass (www.arignabiofuels.ie). This might also be the reason that the correlation coefficient between smokeless coal and peat could reach 0.92. In this regard, it is hard to separate peat and smokeless coal in factor analysis of the ambient dataset. Peat briquettes MS is better correlated with PMF factor BBOA (taken from Ng et al.[43]) (mean R^2=0.88) than dry wood (R^2=0.77) which implies that in areas where peat is widely used (e.g. Ireland and the UK) extreme care is required to separate peat and BBOA since they have similar MS and usually show temporal covariation as domestic heating fuels. Peat shows moderate correlation (mean R^2=0.8) with HOA (taken from Crippa et al.[21]), but elevated signal at *m/z* 60 for peat should be enough to distinguish them in PMF analysis. Wood and HOA shows a bad correlation (mean

255 R^2=0.25) which means that wood burning emissions can be easily separated from HOA in factor
256 analysis of the ambient dataset.

257

258 **Ambient measurement of NR-PM_1 in Galway, Ireland.** An overview of the NR-PM_1
259 components (organics, nitrate, sulfate, and ammonium) in Galway during early winter (from
260 October 17th to November 23rd, 2015) is shown in Figure 2 as well as meteorological parameters
261 (wind direction, wind speed, relative humidity, and temperature). During the measurement
262 period, the temperatures were mild, with an average of 10.6 ± 2.6 ^{o}C ranging from 3 ^{o}C to 16 ^{o}C.
263 The ambient relative humidity had a mean value of 90.8 ± 8.8 %, ranging from 56 % to 100 %.
264 The wind mainly blew from the southwest (46 % of the time) with a mean wind velocity of 3.1 ±
265 1.6 m/s ranging from 0.4 to 9.2 m/s. The ACSM yielded a range of NR-PM_1 concentrations from
266 0.1 to 43.5 μg/m^3, with a low mean value of 3.4 ± 4.5 μg/m^3 mainly due to the frequent influence
267 of clean marine air masses. However, under certain meteorological conditions of continental air
268 masses (periods S1 and S2) and low wind speed (< 2 m/s), a high concentration of NR-PM_1 can
269 build up throughout the day, with an average of 7.8 μg/m^3 and 11.2 μg/m^3 for S1 and S2,
270 respectively. Even with marine air masses and associated low wind speed (M3), high peak NR-
271 PM_1 concentration (34 μg/m^3, 10 times mean NR-PM_1 value) can be seen in the
272 evening/nighttime, indicating the large emissions from domestic heating in Galway. And a very
273 low background concentration of lower than 1 μg/m^3 was observed during the daytime of the
274 period M3 despite high pollution at night. Thus, it is insightful to analyze the composition during
275 different periods.

On average, the NR-PM_1 mass mainly comprised of OA (50%), followed by sulfate (24%), ammonium (13%), and nitrate (13%) for the entire measurement period in Galway (Figure 2d). However, under different meteorological conditions, their fractions vary significantly. During stagnant time periods (S2) with continental air masses, the pollution levels were elevated throughout the day and the fraction of secondary inorganic aerosols (sulfate, nitrate, and ammonium) increased to around 63% (Figure 2e), indicating a regional source. In contrast, during marine time periods, OA alone accounts for 76% of total NR-PM_1 mass (Figure 2f). The recurring evening/nighttime pollution events with OA being the dominant component underline the importance of source apportionment of OA.



285 **Figure 2.** Time series of (a) wind direction (wd) and wind speed (ws); (b) relative humidity (RH)
286 and temperature (T); (c) pressure (P); and (d) submicron species i.e. organics, sulfate,
287 ammonium, and nitrate; inset pie chart shows average composition for the entire study; and pie
288 chart contribution of submicron species during selected periods (e) S2; and (f) M3; The colors

289 and characters on the top of the graph represent the different air masses classifications (light red:
290 stagnant continental (S1 and S2); light green: marine with high wind speed (M1 and M2; dark
291 green: marine with low wind speed (M3); back trajectory analysis for the whole periods is shown
292 in Figure S11).

293 **OA source apportionment.** For source apportionment of OA, we take advantage of ME-2
294 which can direct the PMF analysis to environmentally reasonable solutions by constraining the
295 priori ACSM derived source profiles of peat, coal, and wood, as well as oil (HOA) from Crippa
296 et al.[21] An *a-value* of 0.1 (i.e. 10% variation in profile) was applied due to the fact that most
297 primary OA was freshly-emitted, with peak concentrations occurring at the early nighttime and
298 thus should have small variation from the ACSM derived fingerprints. Due to the lack of
299 possible tracer marker for each type of domestic fuel combustions, the best *a-value* will be
300 further investigated as indicated in Elser et al.[17] As illustrated in Figure 3a, a 5-factor solution
301 including four constrained primary factors and one additional unconstrained OOA is found to be
302 the environmentally reasonable solution. Further increase of the number of factors leads to
303 uninterpretable factors (Figure S7). The time series of four primary factors (Figure 3b) show
304 similar temporal variation due to the similar emission time from domestic heating activities
305 during the evening which was also the reason why ME-2 is necessary to separate pre-constrained
306 factors to estimate the contribution of candidate sources. Otherwise, highly mixed and un-
307 meaningful factors would be achieved with a totally unconstrained PMF (Figure S8) and thus, an
308 unconstrained PMF would be unable to estimate the contribution of the different combustion
309 fuels to the air pollution. In contrast, the OOA could be easily resolved both in constrained and
310 unconstrained PMF due to its time series distinct from primary factors. OOA is characterized
311 with a prominent signal at *m/z* 44 and has a high correlation with sulfate (R^2=0.83). The OOA

time series show a relatively constant high level during periods S1 and S2, indicating the importance of OOA formation under these conditions. However, during periods M1, M2, and M3, some evening peaks of OOA can also be observed, indicating an additional contribution from a more local and evening/nighttime production process. Unlike OOA, the resulting time series of primary factors only show elevated evening/nighttime pollution levels, corresponding to emission time.

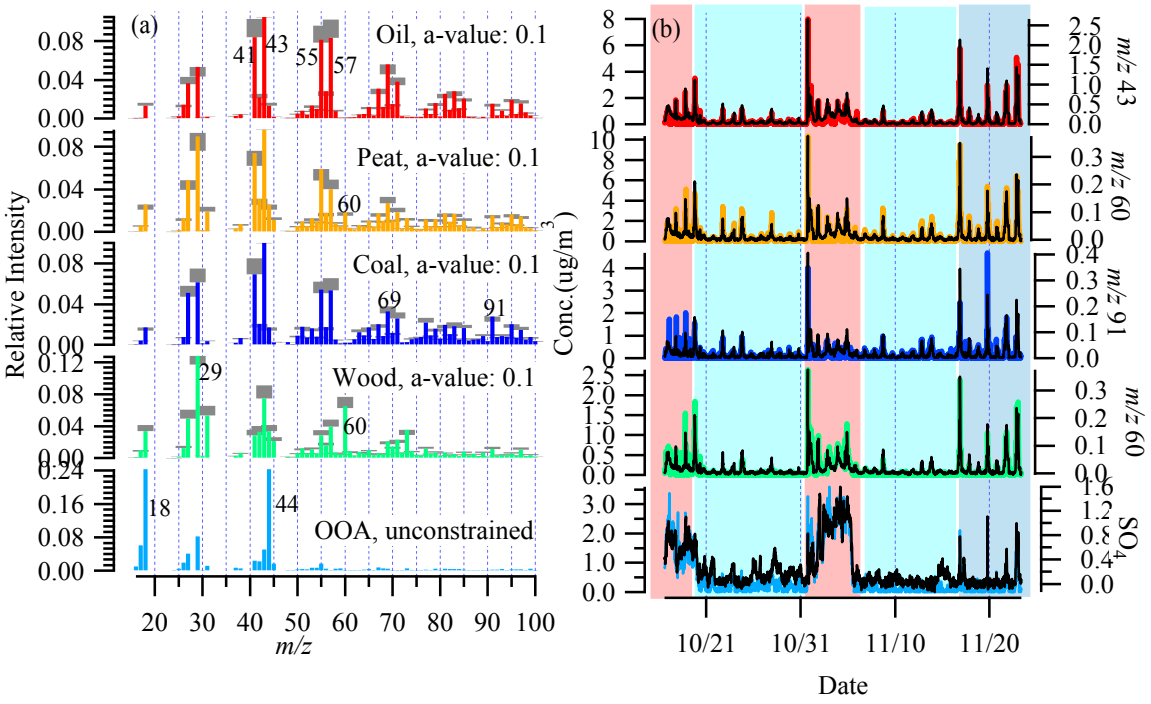


Figure 3. (a) Factor profiles (mass spectra) of 5-factor ME-2 solution. The a-value method within SoFi was applied (matrix with *m/z* up to 100 was used for PMF). Oil burning profile is from ambient data PMF-derived hydrocarbon-like organic aerosol (HOA)[21]. Peat, wood, and coal reference profiles are from previous fingerprinting experiments. Grey bar in the back represents reference profile employed. (b) And the factor time series (color coded with the same periods of

S1, M1, S2, M2, and M3 in Figure 2) of source apportionment and comparison of primary factors with typical ACSM fragments (HOA vs *m/z* 43 (R^2=0.88); Peat vs *m/z* 60 (R^2=0.84); Coal vs *m/z* 91 (R^2=0.63); Wood vs *m/z* 60 (R^2=0.79)) and comparison of secondary factor (OOA) with an external source of sulfate (R^2=0.83).

When running ME-2 using the *a-value* approach on ACSM datasets, the selection of best *a* value is critical. An *a* value that is too small (i.e. very tightly constrained) might not give enough freedom to the unconstrained factor (e.g. OOA) while a large *a* value might lead to inter-factor mixing. Thus, an optimized *a* value need to be explored in ME-2. Previous work by Elser et al.[17] suggests the selection criteria of using factor-tracer correlation to find the best *a* value corresponding solution that best describes the organic aerosols. A combination of different *a* values for a specific factor can be derived using this method. However, in cases where the constrained factors' corresponding tracer data are not available, we assume a same *a* value for all constrained factors. To explore the influence of *a* value, *a* value of 0, 0.05, 0.1, and 0.2 were run in ME-2. The constrained factors' relative fraction and the correlation between the unconstrained OOA and sulfate are found to be affected by *a* value differently (Figure S10). The factors' relative contribution to total OA for oil, coal, and wood burning remain nearly unchanged for this *a* value range (0-0.2). In contrast, OOA fraction decreases sharply from 45% to 35% as *a* value of increases from 0 to 0.1 but slowly from 35% to 34% as *a* value increases from 0.1 to 0.2 while peat burning fraction increases from 21% (*a* value of 0) to 32% (*a* value of 0.1) and decreases to 28% (*a* value of 0.2). R^2 between the OOA and sulfate increases from 0.71 to 0.83 as the *a* value increase from 0 to 0.1 and starts to level off after 0.1. Thus, 0.1 is found to be the most optimized *a* value because it can give enough freedom to OOA and prevent further mixing

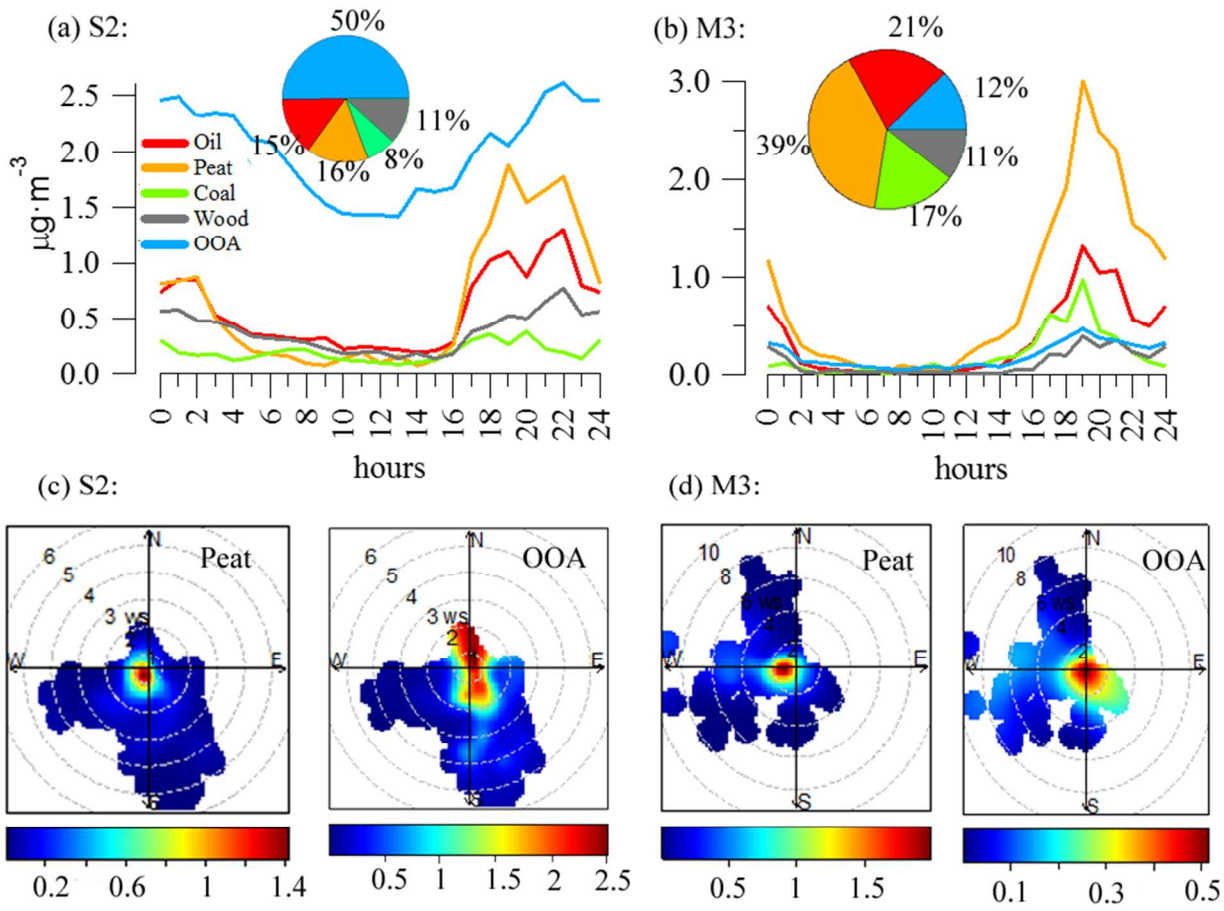
between factors by increasing the *a* value. It is also important to note that peat is always the largest primary fraction with the same *a* value.

Local vs. regional OA sources. During the measurement periods, the frequent marine air masses bring a very clean background OA level (<0.1 μg/m^3) which provide a perfect chance to study the anthropogenic pollutants especially for the local sources. In addition, occasional continental air masses bring the opportunity to study the regional OA sources from the UK and/or mainland Europe. The relationship between resolved OA factors and meteorology is, therefore, demonstrated by comparing two distinct pollution patterns corresponding to continental and marine air masses (Figure S11). Continental air masses and marine air masses alternated during the measurement period and led to different contributions of OA factors, as well as diurnal patterns especially for OOA. As shown in Figure 4 (a), OOA is the major component of OA in continental air masses (S2; 50%), and its diurnal cycle shows higher concentration during the night than day which might be due to the influence of planetary boundary layer that's shallower during night and higher during the day. Wind roses of OOA during S2 show that higher OOA concentrations are related to air masses from the north and southeast side rather than the west side of measurement location, indicating its origin might come from mainland Europe or the UK rather than the ocean (Figure 4c). In contrast, in the marine air masses (i.e. M3 period), OOA only comprises 12% of total OA (Figure 4b), and the diurnal cycle of it shows a peak at evening/nighttime which coincides with primary factors, indicating a possible nighttime OOA formation process of the condensation of semi-volatile organic matter emitted from fuel combustion[47]. In addition, the wind roses of OOA (Figure 4d) during M3 show no preference for wind direction but for low wind speed which might be required for the formation process as semi-volatile organic matter dissipate more quickly with

high wind speed. The wind rose of OOA between S2 and M3 shows a clear different pattern indicating the difference in transport and formation of OOA under different meteorological conditions. Similarly, inorganic aerosols (sulfate, nitrate, and ammonium) also show obvious peaks during M3 nighttime which should also come from primary emissions or fast night time formation (Figure 2).

Unlike OOA, all primary factors (oil, peat, coal, and wood burning), show peak concentrations at early night (at around 19:00) and very low concentrations (<0.5 $\mu g/m^3$) during the day (8:00-16:00, sunrise at around 8:00 and sunset at around 16:00 during the measurement period), corresponding to their emission time and locally produced nature. Primary OA contributes around 50 % during S2 and 88% during M3, indicating its importance for air pollution over the wintertime, especially during marine periods. Peat burning contributes 39% during M3 and 16% during S2 (Figure 4a and 4b), making it the largest primary contributor to the total ambient OA during cold winter nights in Galway. This is in great contrast to the relatively small usage of peat as indicated by the census data (Figure S1) from Central Statistics Office which shows only around 10% of the non-natural gas and non-electricity households use peat for heating. However, the emission factor profile (Table S1)[45] which indicates a large emission factor and a low net calorific value for peat can help explain the dominance of peat. Similarly, smoky coal has a large emission factor and claim for 17% of total OA mass during M3 when less than 1% of the households report the use of smoky coal for heating probably due to the ban on coal in Galway. In contrast, most households use oil for heating (around 85%), but due to the low emission factor for oil burning, a relatively small fraction (21% during M3) is observed. HOA is usually used to quantify the traffic emissions.[21] However, the time series of HOA in this study show a huge early evening peak (at around 19:00) and absence of a morning rush hour peak (Figure 4a and 4b),

391 which points to its major source from domestic heating activities rather than traffic as reported
392 by previous papers.[34, 35] It is possible that the interference from oil burning due to their similar
393 mass spectra[22,23] and the low mass resolution of ACSM leads to the difficulties in resolving the
394 traffic factor with a low contribution (e.g. <5%), in particular when it co-varies with a source
395 with higher emissions. Previous work by Ulbrich et al. suggests that true components with <5%
396 of the mass are hard to be retrieved accurately using PMF.[46] In contrast to OOA, the wind roses
397 of major primary factor (i.e. peat burning) always show an origin from the west of the
398 measurement site during both S2 and M3 periods which is consistent with the location of the
399 residential area.



400 **Figure 4.** Diurnal cycle of resolved factors (i.e. oil, peat, coal, wood, and OOA) during periods
401 (a) of relatively stagnant and continental air masses (S2) and (b) marine air masses (M3) (insets
402 are relative contribution of the resolved OA factors); Polar plot of hourly averaged major
403 component of OA (i.e. peat and OOA; color coded based on concentration of each species in
404 μg/m^3) as function of wind speed (radial axis) and wind direction during periods (c) S2 and (d)
405 M3. Polar plots figures were generated with OpenAir software[48].

406 ASSOCIATED CONTENT

407 **Supporting Information**. Scheme S1 shows combustion and sampling system for solid fuels
408 using ACSM. Figure S1 shows the households by the type of central heating (oil, peat, coal, and

409 wood) from Central Statistics Office, 2011. Table S1 provides the emission factors and caloric
410 values for oil, peat, coal, and wood. Table S2 provides correlation coefficient (R^2) between
411 ACSM profiles of different sources and PMF factors. Figure S2 shows the relative fraction of
412 ACSM measured species (i.e. organics, sulfate, nitrate, ammonium, and chloride). Figures S3-S5
413 show the mass spectra of each type of fuel under different states. Figure S6 provides relative
414 difference of dry wood and smoky coal MS profile compared to peat at each m/z. Figures S7-S9
415 provide the time series and mass spectra of PMF solutions. Figure S10 provides the relative
416 contribution of the resolved factors and correlation between OOA and sulfate with different *a*
417 values (0-0.2). Figure S11 shows the back trajectory during the measurement period in Galway
418 Ireland. This material is available free of charge via the Internet at http://pubs.acs.org.

419 AUTHOR INFORMATION

420 **Corresponding Author**

421 *Ru-Jin Huang, Phone: +86-(0)29-6233-6275; Email: rujin.huang@ieecas.cn

422 *Colin O'Dowd, Phone: +353-91-49-3306; Email: colin.odowd@nuigalway.ie

423 **Notes**

424 The authors declare no competing financial interest.

425 ACKNOWLEDGMENT

426 This work was supported by EPA-Ireland (AEROSOURCE, 2016-CCRP-MS-31), the National
427 Natural Science Foundation of China (NSFC) under Grant No. 91644219, and Chinese
428 Scholarship Council (CSC, No. 201506310020). We would also like to thank Harry Arndt for
429 allowing us to use the cottage in County Tipperary for the burning experiments, and especially

for providing valuable input into the design and construction of the sampling system. The team from University College Cork would like to acknowledge support from the Environmental Protection Agency and Department of Environment Community and Local Government in Ireland through the SAPPHIRE project (2013-EH-MS.15).

REFERENCES

1. Pope, I. C.; Burnett, R. T.; Thun, M. J., Lung cancer, cardiopulmonary mortality, and long-term exposure to fine particulate air pollution. *JAMA* **2002,** *287*, (9), 1132-1141.

2. Sandström, T.; Nowak, D.; van Bree, L., Health effects of coarse particles in ambient air: messages for research and decision-making. *Eur. Respir. J.* **2005,** *26*, (2), 187-188.

3. O'Dowd, C. D.; Facchini, M. C.; Cavalli, F.; Ceburnis, D.; Mircea, M.; Decesari, S.; Fuzzi, S.; Yoon, Y. J.; Putaud, J.-P., Biogenically driven organic contribution to marine aerosol. *Nature* **2004,** *431*, (7009), 676-680.

4. Kelly, I.; Clancy, L., Mortality in a general hospital and urban air pollution. *Irish Med. J.* **1984,** *77*, (10), 322-324.

5. Clancy, L.; Goodman, P.; Sinclair, H.; Dockery, D. W., Effect of air-pollution control on death rates in Dublin, Ireland: an intervention study. *Lancet* **2002,** *360*, (9341), 1210-1214.

6. Goodman, P. G.; Rich, D. Q.; Zeka, A.; Clancy, L.; Dockery, D. W., Effect of Air Pollution Controls on Black Smoke and Sulfur Dioxide Concentrations across Ireland. *J. Air & Waste Manage.* **2009,** *59*, (2), 207-213.

449 7. Kourtchev, I.; Hellebust, S.; Bell, J. M.; O'Connor, I. P.; Healy, R. M.; Allanic, A.;
450 Healy, D.; Wenger, J. C.; Sodeau, J. R., The use of polar organic compounds to estimate the
451 contribution of domestic solid fuel combustion and biogenic sources to ambient levels of organic
452 carbon and PM2.5 in Cork Harbour, Ireland. *Sci. Total Environ.* **2011,** *409*, (11), 2143-2155.

453 8. International Energy Agency, 2013. Energy balance for Ireland website;

454 http://www.iea.org/statistics/statisticssearch/report/?country=IRELAND&product=Coal&year=2
455 013 (last access: December 2016).

456 9. Wang, X.; Williams, B.; Wang, X.; Tang, Y.; Huang, Y.; Kong, L.; Yang, X.; Biswas, P.,
457 Characterization of organic aerosol produced during pulverized coal combustion in a drop tube
458 furnace. *Atmos. Chem. Phys.* **2013,** *13*, (21), 10919-10932.

459 10. Weimer, S.; Alfarra, M. R.; Schreiber, D.; Mohr, M.; Prévôt, A. S. H.; Baltensperger, U.,
460 Organic aerosol mass spectral signatures from wood-burning emissions: Influence of burning
461 conditions and type. *J. Geophys. Res-Atmos.* **2008,** *113*, (10), 304-305.

462 11. Zhou, W.; Jiang, J.; Duan, L.; Hao, J., Evolution of Submicrometer Organic Aerosols
463 during a Complete Residential Coal Combustion Process. *Environ. Sci. Technol.* **2016**, *50* (14),
464 7861–7869.

465 12. Jayne, J. T.; Leard, D. C.; Zhang, X.; Davidovits, P.; Smith, K. A.; Kolb, C. E.; Worsnop,
466 D. R., Development of an aerosol mass spectrometer for size and composition analysis of
467 submicron particles. *Aerosol Sci. Technol.* **2000,** *33*, (1-2), 49-70.

13. Canagaratna, M. R.; Jayne, J. T.; Jimenez, J. L.; Allan, J. D.; Alfarra, M. R.; Zhang, Q.; Onasch, T. B.; Drewnick, F.; Coe, H.; Middlebrook, A.; Delia, A.; Williams, L. R.; Trimborn, A. M.; Northway, M. J.; DeCarlo, P. F.; Kolb, C. E.; Davidovits, P.; Worsnop, D. R., Chemical and microphysical characterization of ambient aerosols with the aerodyne aerosol mass spectrometer. *Mass Spectrom. Rev.* **2007,** *26*, (2), 185-222.

14. Middlebrook, A. M.; Bahreini, R.; Jimenez, J. L.; Canagaratna, M. R., Evaluation of Composition-Dependent Collection Efficiencies for the Aerodyne Aerosol Mass Spectrometer using Field Data. *Aerosol Sci. Technol.* **2012,** *46*, (3), 258-271.

15. Carbone, S.; Saarikoski, S.; Frey, A.; Reyes, F.; Reyes, P.; Castillo, M.; Gramsch, E.; Oyola, P.; Jayne, J.; Worsnop, D.; Hillamo, R., Chemical characterization of submicron Aerosol particles in Santiago de Chile. *Aerosol Air Qual. Res.* **2013,** *13*, (2), 462-473.

16. Canonaco, F.; Slowik, J. G.; Baltensperger, U.; Prévôt, A. S. H., Seasonal differences in oxygenated organic aerosol composition: Implications for emissions sources and factor analysis. *Atmos. Chem. Phys.* **2015,** *15*, (12), 6993-7002.

17. Elser, M.; Huang, R. J.; Wolf, R.; Slowik, J. G.; Wang, Q.; Canonaco, F.; Li, G.; Bozzetti, C.; Daellenbach, K. R.; Huang, Y.; Zhang, R.; Li, Z.; Cao, J.; Baltensperger, U.; El-Haddad, I.; André, P., New insights into PM2.5 chemical composition and sources in two major cities in China during extreme haze events using aerosol mass spectrometry. *Atmos. Chem. Phys.* **2016,** *16*, (5), 3207-3225.

487 18. Zhang, Q.; Jimenez, J. L.; Canagaratna, M. R.; Ulbrich, I. M.; Ng, N. L.; Worsnop, D. R.;
488 Sun, Y., Understanding atmospheric organic aerosols via factor analysis of aerosol mass
489 spectrometry: A review. *Anal. Bioanal. Chem.* **2011,** *401*, (10), 3045-3067.

490 19. Jimenez, J. L.; Canagaratna, M. R.; Donahue, N. M.; Prevot, A. S. H.; Zhang, Q.; Kroll,
491 J. H.; DeCarlo, P. F.; Allan, J. D.; Coe, H.; Ng, N. L.; Aiken, A. C.; Docherty, K. S.; Ulbrich, I.
492 M.; Grieshop, A. P.; Robinson, A. L.; Duplissy, J.; Smith, J. D.; Wilson, K. R.; Lanz, V. A.;
493 Hueglin, C.; Sun, Y. L.; Tian, J.; Laaksonen, A.; Raatikainen, T.; Rautiainen, J.; Vaattovaara, P.;
494 Ehn, M.; Kulmala, M.; Tomlinson, J. M.; Collins, D. R.; Cubison, M. J.; E.; Dunlea, J.;
495 Huffman, J. A.; Onasch, T. B.; Alfarra, M. R.; Williams, P. I.; Bower, K.; Kondo, Y.; Schneider,
496 J.; Drewnick, F.; Borrmann, S.; Weimer, S.; Demerjian, K.; Salcedo, D.; Cottrell, L.; Griffin, R.;
497 Takami, A.; Miyoshi, T.; Hatakeyama, S.; Shimono, A.; Sun, J. Y.; Zhang, Y. M.; Dzepina, K.;
498 Kimmel, J. R.; Sueper, D.; Jayne, J. T.; Herndon, S. C.; Trimborn, A. M.; Williams, L. R.;
499 Wood, E. C.; Middlebrook, A. M.; Kolb, C. E.; Baltensperger, U.; Worsnop, D. R., Evolution of
500 Organic Aerosols in the Atmosphere. *Science* **2009,** *326*, (5959), 1525-1529.

501 20. Lanz, V. A.; Prévôt, A. S. H.; Alfarra, M. R.; Weimer, S.; Mohr, C.; Decarlo, P. F.;
502 Gianini, M. F. D.; Hueglin, C.; Schneider, J.; Favez, O.; D'Anna, B.; George, C.; Baltensperger,
503 U., Characterization of aerosol chemical composition with aerosol mass spectrometry in Central
504 Europe: An overview. *Atmos. Chem. Phys.* **2010,** *10*, (21), 10453-10471.

505 21. Crippa, M.; Decarlo, P. F.; Slowik, J. G.; Mohr, C.; Heringa, M. F.; Chirico, R.; Poulain,
506 L.; Freutel, F.; Sciare, J.; Cozic, J.; Di Marco, C. F.; Elsasser, M.; Nicolas, J. B.; Marchand, N.;
507 Abidi, E.; Wiedensohler, A.; Drewnick, F.; Schneider, J.; Borrmann, S.; Nemitz, E.;
508 Zimmermann, R.; Jaffrezo, J. L.; Prévôt, A. S. H.; Baltensperger, U., Wintertime aerosol

509 chemical composition and source apportionment of the organic fraction in the metropolitan area
510 of Paris. *Atmos. Chem. Phys.* **2013,** *13*, (2), 961-981.

511 22. Canagaratna, M. R.; Jayne, J. T.; Ghertner, D. A.; Herndon, S.; Shi, Q.; Jimenez, J. L.;
512 Silva, P. J.; Williams, P.; Lanni, T.; Drewnick, F.; Demerjian, K. L.; Kolb, C. E.; Worsnop, D.
513 R., Chase Studies of Particulate Emissions from in-use New York City Vehicles. *Aerosol Sci.*
514 *Technol.* **2004,** *38*, (6), 555-573.

515 23. Schneider, J.; Weimer, S.; Drewnick, F.; Borrmann, S.; Helas, G.; Gwaze, P.; Schmid,
516 O.; Andreae, M. O.; Kirchner, U., Mass spectrometric analysis and aerodynamic properties of
517 various types of combustion-related aerosol particles. *Int. J. Mass Spectrom.* **2006,** *258*, (1-3),
518 37-49.

519 24. He, L. Y.; Lin, Y.; Huang, X. F.; Guo, S.; Xue, L.; Su, Q.; Hu, M.; Luan, S. J.; Zhang, Y.
520 H., Characterization of high-resolution aerosol mass spectra of primary organic aerosol
521 emissions from Chinese cooking and biomass burning. *Atmos. Chem. Phys.* **2010,** *10*, (23),
522 11535-11543.

523 25. Healy, R. M.; Hellebust, S.; Kourtchev, I.; Allanic, A.; O'Connor, I. P.; Bell, J. M.;
524 Healy, D. A.; Sodeau, J. R.; Wenger, J. C., Source apportionment of PM_{2.5} in Cork
525 Harbour, Ireland using a combination of single particle mass spectrometry and quantitative semi-
526 continuous measurements. *Atmos. Chem. Phys.* **2010,** *10*, (19), 9593-9613.

527 26. Dall'Osto, M.; Ovadnevaite, J.; Ceburnis, D.; Martin, D.; Healy, R. M.; O'Connor, I. P.;
528 Kourtchev, I.; Sodeau, J. R.; Wenger, J. C.; O'Dowd, C., Characterization of urban aerosol in

529 Cork city (Ireland) using aerosol mass spectrometry. *Atmos. Chem. Phys.* **2013,** *13*, (9), 4997-
530 5015.

531 27. Ng, N. L.; Herndon, S. C.; Trimborn, A.; Canagaratna, M. R.; Croteau, P. L.; Onasch, T.
532 B.; Sueper, D.; Worsnop, D. R.; Zhang, Q.; Sun, Y. L.; Jayne, J. T., An Aerosol Chemical
533 Speciation Monitor (ACSM) for Routine Monitoring of the Composition and Mass
534 Concentrations of Ambient Aerosol. *Aerosol Sci. Technol.* **2011,** *45*, (7), 780-794.

535 28. Eaton, J. M.; McGoff, N. M.; Byrne, K. A.; Leahy, P.; Kiely, G., Land cover change and
536 soil organic carbon stocks in the Republic of Ireland 1851–2000. *Climatic Change* **2008,** *91*, (3-
537 4), 317-334.

538 29. Canonaco, F.; Crippa, M.; Slowik, J. G.; Baltensperger, U.; Prévôt, A. S. H., SoFi, an
539 IGOR-based interface for the efficient use of the generalized multilinear engine (ME-2) for the
540 source apportionment: ME-2 application to aerosol mass spectrometer data. *Atmos. Meas. Tech.*
541 **2013,** *6*, (12), 3649-3661.

542 30. Paatero, P., Least squares formulation of robust non-negative factor analysis. *Chemometr.*
543 *Intell. Lab* **1997,** *37*, (1), 23-35.

544 31. Paatero, P.; Eberly, S.; Brown, S. G.; Norris, G. A., Methods for estimating uncertainty in
545 factor analytic solutions. *Atmos. Meas. Tech.* **2014,** *7*, (3), 781-797.

546 32. Lanz, V. A.; Alfarra, M. R.; Baltensperger, U.; Buchmann, B.; Hueglin, C.; Prévôt, A. S.
547 H., Source apportionment of submicron organic aerosols at an urban site by factor analytical
548 modelling of aerosol mass spectra. *Atmos. Chem. Phys.* **2007,** *7*, (6), 1503-1522.

549 33. Crippa, M.; Canonaco, F.; Lanz, V. A.; Äijälä, M.; Allan, J. D.; Carbone, S.; Capes, G.;
550 Ceburnis, D.; Dall'Osto, M.; Day, D. A.; DeCarlo, P. F.; Ehn, M.; Eriksson, A.; Freney, E.;
551 Hildebrandt Ruiz, L.; Hillamo, R.; Jimenez, J. L.; Junninen, H.; Kiendler-Scharr, A.;
552 Kortelainen, A. M.; Kulmala, M.; Laaksonen, A.; Mensah, A. A.; Mohr, C.; Nemitz, E.;
553 O'Dowd, C.; Ovadnevaite, J.; Pandis, S. N.; Petäjä, T.; Poulain, L.; Saarikoski, S.; Sellegri, K.;
554 Swietlicki, E.; Tiitta, P.; Worsnop, D. R.; Baltensperger, U.; Prévôt, A. S. H., Organic aerosol
555 components derived from 25 AMS data sets across Europe using a consistent ME-2 based source
556 apportionment approach. *Atmos. Chem. Phys.* **2014,** *14*, (12), 6159-6176.

557 34. Petit, J. E.; Favez, O.; Sciare, J.; Canonaco, F.; Croteau, P.; Močnik, G.; Jayne, J.;
558 Worsnop, D.; Leoz-Garziandia, E., Submicron aerosol source apportionment of wintertime
559 pollution in Paris, France by double positive matrix factorization (PMF2) using an aerosol
560 chemical speciation monitor (ACSM) and a multi-wavelength Aethalometer. *Atmos. Chem. Phys.*
561 **2014,** *14*, (24), 13773-13787.

562 35. Poulain, L.; Iinuma, Y.; Müller, K.; Birmili, W.; Weinhold, K.; Brüggemann, E.; Gnauk,
563 T.; Hausmann, A.; Löschau, G.; Wiedensohler, A.; Herrmann, H., Diurnal variations of ambient
564 particulate wood burning emissions and their contribution to the concentration of Polycyclic
565 Aromatic Hydrocarbons (PAHs) in Seiffen, Germany. *Atmos. Chem. Phys.* **2011,** *11*, (24),
566 12697-12713.

567 36. Central statistical office 2011, Ireland website;

568 http://www.cso.ie/px/pxeirestat/Statire/SelectVarVal/Define.asp?Maintable=CDD41&Planguage
569 =0 (last access: December 2016).

570 37. Alfarra, M. R.; Prevot, A. S. H.; Szidat, S.; Sandradewi, J.; Weimer, S.; Lanz, V. A.;
571 Schreiber, D.; Mohr, M.; Baltensperger, U., Identification of the mass spectral signature of
572 organic aerosols from wood burning emissions. *Environ. Sci. Technol.* **2007,** *41*, (16), 5770-
573 5777.

574 38. Duplissy, J.; DeCarlo, P. F.; Dommen, J.; Alfarra, M. R.; Metzger, A.; Barmpadimos, I.;
575 Prevot, A. S. H.; Weingartner, E.; Tritscher, T.; Gysel, M.; Aiken, A. C.; Jimenez, J. L.;
576 Canagaratna, M. R.; Worsnop, D. R.; Collins, D. R.; Tomlinson, J.; Baltensperger, U., Relating
577 hygroscopicity and composition of organic aerosol particulate matter. *Atmos. Chem. Phys.* **2011,**
578 *11*, (3), 1155-1165.

579 39. Allan, J. D.; Delia, A. E.; Coe, H.; Bower, K. N.; Alfarra, M. R.; Jimenez, J. L.;
580 Middlebrook, A. M.; Drewnick, F.; Onasch, T. B.; Canagaratna, M. R.; Jayne, J. T.; Worsnop, D.
581 R., A generalised method for the extraction of chemically resolved mass spectra from Aerodyne
582 aerosol mass spectrometer data. *J. Aerosol Sci.* **2004,** *35*, (7), 909-922.

583 40. Allan, J. D.; Jimenez, J. L.; Williams, P. I.; Alfarra, M. R.; Bower, K. N.; Jayne, J. T.;
584 Coe, H.; Worsnop, D. R., Quantitative sampling using an Aerodyne aerosol mass spectrometer 1.
585 Techniques of data interpretation and error analysis. *J. Geophys. Res-Atmos.* **2003,** *108*, (D3),
586 4090-4091.

587 41. Budisulistiorini, S. H.; Riva, M.; Williams, M.; Chen, J.; Itoh, M.; Surratt, J. D.; Kuwata, M.,
588 Light-Absorbing Brown Carbon Aerosol Constituents from Combustion of Indonesian Peat and
589 Biomass. *Environ. Sci. Technol.* **2017,** 51, (8), 4415-4423.

590 42. Szajdak, L.; Brandyk, T.; Szatylowicz, J., Chemical properties of different peat-moorsh
591 soils from the Biebrza River Valley. *Agronomy Res.* **2007,** *5*, (2), 165-174.

592 43. Ng, N. L.; Canagaratna, M. R.; Zhang, Q.; Jimenez, J. L.; Tian, J.; Ulbrich, I. M.; Kroll,
593 J. H.; Docherty, K. S.; Chhabra, P. S.; Bahreini, R.; Murphy, S. M.; Seinfeld, J. H.; Hildebrandt,
594 L.; Donahue, N. M.; DeCarlo, P. F.; Lanz, V. A.; Prévôt, A. S. H.; Dinar, E.; Rudich, Y.;
595 Worsnop, D. R., Organic aerosol components observed in Northern Hemispheric datasets from
596 Aerosol Mass Spectrometry. *Atmos. Chem. Phys.* **2010,** *10*, (10), 4625-4641.

597 44. Ibarra, J.; Munoz, E.; Moliner, R., FTIR study of the evolution of coal structure during
598 the coalification process. *Org. Geochem.* **1996,** *24*, (6), 725-735.

599 45. TNO 2001: TNO Institute of Environmental Sciences, Energy Research and Process
600 Innovations: CEPMEIP Database, available at http://www.air.sk/tno/cepmeip, Apeldoorn 2001
601 (last access: December 2016).

602 46. Ulbrich, I. M.; Canagaratna, M. R.; Zhang, Q.; Worsnop, D. R.; Jimenez, J. L., Interpretation
603 of organic components from Positive Matrix Factorization of aerosol mass spectrometric data.
604 *Atmos. Chem. Phys.* **2009,** *9*, (9), 2891-2918.

605 47. Tiitta, P.; Leskinen, A.; Hao, L.; Yli-Pirilä, P.; Kortelainen, M.; Grigonyte, J.; Tissari, J.;
606 Lamberg, H.; Hartikainen, A.; Kuuspalo, K.; Kortelainen, A. M.; Virtanen, A.; Lehtinen, K. E.
607 J.; Komppula, M.; Pieber, S.; Prévôt, A. S. H.; Onasch, T. B.; Worsnop, D. R.; Czech, H.;
608 Zimmermann, R.; Jokiniemi, J.; Sippula, O., Transformation of logwood combustion emissions
609 in a smog chamber: formation of secondary organic aerosol and changes in the primary organic
610 aerosol upon daytime and nighttime aging. *Atmos. Chem. Phys.* **2016,** *16*, (20), 13251-13269.

48. Carslaw, D. C.; Ropkins, K., openair — An R package for air quality data analysis. *Environ. Modell. Softw.* **2012,** *27–28*, 52-61.

TOC:

